

# Effect of Shape Anisotropy on Stop-Band Response of Fe and Permalloy Based Tunable Microstrip Filters

Bijoy Kuanr, R. E. Camley, and Z. Celinski

**Abstract**—The magnetic/dielectric hybrid transmission line structures provide a new class of microwave/millimeter wave devices, useful for signal processing. Reduction of device dimensions in these magnetic monolithic microwave integrated circuits (M-MMICs) is important from the cost and reliability point of view. Here, we explore the transmission characteristics of Fe and Permalloy based microstrip filters with microstrips of different widths, lengths, and thicknesses. The gyromagnetic resonance occurs at microwave frequencies of up to 12 GHz for Fe and 5 GHz for Permalloy, even in the absence of any dc magnetic field. The resulting absorption yields the stop-band behavior of the device. Our microstrip geometry significantly boosts the operational frequency due to an induced shape-anisotropy. Different geometries induce different demagnetization factors and hence different resonance frequencies. We calculate the frequency-boosting characteristics of the devices due to induced shape-anisotropy and observed a good match to our measurements.

**Index Terms**—Shape anisotropy, stop-band filters.

## I. INTRODUCTION

THERE is now considerable interest in the development of micromagnetic devices using metallic magnetic films grown on semiconducting substrates [1]–[9]. These magnetic/dielectric hybrid transmission line structures promise a new class of microwave/millimeter wave devices, which could be useful for high-frequency signal processing. Integration of planar microstrip devices with ferromagnetic films is of considerable interest for microwave and millimeter-wave applications, e.g., stop-band and pass-band filters, magnetic switches, quarter wave length lines, etc. The stop-band devices rely on the absorption of microwave energy at ferromagnetic resonance (FMR) [1]–[9]. In all these applications, the use of a magnetic material with high permeability at microwave frequencies is essential for satisfactory performance.

Most of the previous devices have been fabricated using molecular beam epitaxy (MBE) [1]–[3]. However, MBE growth is incompatible with the standard integrated circuit technologies. We have explored the use of two metallic ferromagnets grown by sputtering for use in microstrip devices—Permalloy (Py) and iron. Permalloy has an advantage, because it has narrow linewidths, has been extensively studied, and is widely used in the industry. It can work up to few gigahertz frequencies with a very low static applied magnetic field. Iron, on the other

hand, has the advantage of a higher saturation magnetization; therefore it can operate at much higher frequencies, compared to Permalloy, for the same applied field. Unfortunately, the larger linewidths and higher conductivity in Fe can lead to unwanted losses at microwave frequencies. However, structures utilizing thin Fe films minimize conduction loss while still producing high attenuation at the band-stop frequency [1].

We have recently constructed [3], [6], [9] band-stop microstrip filters using Py and Fe as the active elements. In this paper, we explore how the geometry of the microstrip can influence the band-stop frequency.

## II. EXPERIMENT

All our devices are prepared on GaAs substrates, the material of choice for high-speed electronics. We deposited the following sequence of materials by sputtering [9]. The bottom electrode of a 2  $\mu\text{m}$  thick Ag layer was grown on top of a 5 nm thick Ti layer (to ensure good adhesion). The rest of the structure is grown through a shadow mask, starting with a thin Ti film for adhesion, then a 4  $\mu\text{m}$  thick  $\text{SiO}_2$  film, Fe or Permalloy film of 0.3 to 0.35  $\mu\text{m}$  thick, followed by a thick Ag film of 2  $\mu\text{m}$  for the top electrode. The FMR linewidth on unpatterned samples was measured at 10 GHz and is 80 Oe for Py and 160 Oe for Fe. The device is patterned by photolithography and dry etched. This produces a long narrow magnetic ribbon, the upper portion of the microstrip, and it is the geometry of the magnetic material that will influence the operational frequency.

We determine the performance of our devices using a vector network analyzer. We characterized [3], [6] the microstrip transmission lines at frequencies from 1 to 40 GHz using an automated vector network analyzer, and a microprobe station. The on wafer through-open-line (TOL) calibration using NIST Multical software [10] ensures the removal of coaxial-to-microstrip transition losses, losses due to electronic components and cables etc. Therefore, the studied transmission coefficient is the true forward  $S_{21}$  scattering term of the filter.

As we will see, the frequency of operation will be significantly altered by changing the geometry—thickness ( $t$ ), width ( $W$ ) and length ( $L$ )—of the magnetic element in the microstrip. The magnetic material is in the form of a long ribbon with the following dimensions: lengths  $L$  of 2.2., 3.3, and 6.6 mm; widths  $W$  of 12, 18, and 26  $\mu\text{m}$ ; and thicknesses  $t$  of 0.3 to 0.35  $\mu\text{m}$ . A static magnetic field  $H$  is applied in the  $z$  direction along the length of the microstrip. The microstrip is operated in a transverse magnetic (TM) mode so a fluctuating microwave magnetic field  $h_{\text{rf}}$  is oriented perpendicular to the static field and parallel to the width of the microstrip in the  $y$  direction. This arrangement ensures a strong interaction between the microwave energy and the ferromagnetic film.

Manuscript received October 15, 2003. This work was supported by the U.S. Army Research Office under grants DAAD19-02-1-0174, DAAD19-00-1-0146, WG11NF-04-1-0247, and by AFOSR project 453-6901 administrated by NISSC.

The authors are with the Center for Magnetism and Magnetic Nanostructures, Physics, University of Colorado at Colorado Springs, Colorado Springs, CO 80933-7150 USA.

Digital Object Identifier 10.1109/TMAG.2004.834197

TABLE I  
COMPARISON OF EXPERIMENTAL AND THEORETICAL RESULTS FOR FMR FREQUENCIES AS A FUNCTION OF (A) LINE WIDTH AND (B) LINE LENGTH.  $W$  IS IN MICROMETERS,  $L$  IS IN MILLIMETERS, AND FMR FREQUENCIES ARE IN GIGAHERTZ. FOR THE THEORETICAL CALCULATIONS, WE TOOK THE THICKNESS EQUAL TO  $0.3 \mu\text{m}$ . FOR PERMALLOY  $\gamma = 2.85 \text{ GHz/kOe}$  AND  $4\pi M_s = 10 \text{ kG}$ . FOR Fe  $\gamma = 2.85 \text{ GHz/kOe}$  AND  $4\pi M_s = 21 \text{ kG}$

(A) $L=3.3 \text{ mm}$					
		Permalloy at $H = 0.08 \text{ kOe}$		Iron at $H = 0.58 \text{ kOe}$	
$W$	$N_y$	FMR (exp.)	FMR (The.)	FMR (exp.)	FMR (The.)
12	0.0413	6.204	6.22	15.32	15.60
18	0.0297	5.28	5.47	14.2	14.31
26	0.0219	4.87	4.89	13.3	13.35
(B) $W=26 \text{ micron}$					
		Permalloy at $H = 0.23 \text{ kOe}$		Iron at $H = 0.44 \text{ kOe}$	
$L$	$N_y$	FMR (exp.)	FMR (The.)	FMR (exp.)	FMR (The.)
2.2	0.02187	5.83	6.04	12.58	12.38
3.3	0.02188	5.88	6.04	12.48	12.38
6.6	0.02189	6.38	6.04	12.68	12.38

### III. RESULTS AND DISCUSSION

Before we present our results, we estimate the effect of the shape anisotropy on the operational frequency. As the magnetization precesses, dynamic magnetic poles are generated at the surfaces and sides of the ferromagnetic ribbon. This leads to dynamic demagnetizing fields which can influence the precession frequency. The theoretical resonance frequency for a ribbon shaped magnetic element is calculated from the following resonance condition [11]:

$$f = \gamma \sqrt{(H + H_a + (N_y - N_z)4\pi M_s)(H + H_a + (N_x - N_z)4\pi M_s)}. \quad (1)$$

The frequency depends on the material properties, such as saturation magnetization  $M_s$ , anisotropy fields  $H_a$ , the gyromagnetic ratio  $\gamma$ , and the magnitude of an applied field  $H$ , assumed to be along a uniaxial anisotropy axis. The demagnetizing factors  $N_x$ ,  $N_y$ , and  $N_z$  may be approximated for a rectangular parallelepiped using an analytical approach developed by Aharoni [12].  $N_x$  is the demagnetizing factor governing the demagnetizing fields perpendicular to the surface of the microstrip,  $N_z$  governs the demagnetizing fields along the length of the microstrip and  $N_y$  is associated with the demagnetizing fields along the width of the microstrip.

For an extended film  $N_x = 1$  and  $N_y = N_z = 0$ , one finds the usual ferromagnetic resonance condition for a thin film:

$$f = \gamma \sqrt{(H + H_a)(H + H_a + 4\pi M_s)}. \quad (2)$$

In the absence of anisotropy fields, the operational frequency is zero at zero applied field. In contrast, we observed a resonance frequency of about 4 GHz for the Py based devices and a resonance frequency of up to 11 GHz for the Fe based devices. This is a substantial boost in operational frequency of

a planar microwave device. This boost could be caused by internal anisotropy fields or by shape anisotropy, and it is necessary to examine different geometries to determine the correct explanation.

In the microstrip geometry,  $N_x \approx 1 - N_y$  and  $N_z \approx 0$ . The important difference between the film geometry and the microstrip geometry is that  $N_y$  is not zero in the microstrip. This increase in the value of  $N_y$  ultimately leads to an increase in the operational frequency over that predicted by thin film resonance condition (2). The values of  $N_y$  are given in Table I for the different geometrical structures, and we will see that the changes in demagnetizing factors completely explain the shifts in resonance frequency and that there is no need to invoke internal anisotropy fields.

The stop-band frequencies for Py and Fe structures with different linewidths and line-lengths are shown in Figs. 1 and 2, respectively at a fixed static magnetic field. It is clear from Fig. 1 that a narrower strip width results in a higher FMR frequency. This is consistent with theoretical expectations since  $N_y$  increases as the strip width decreases, thereby increasing the resonance frequency. It is interesting to note that the linewidth shows no clear pattern as a function of the width of the magnetic element. In fact, the widest microstrips seem to have the largest linewidths. The insertion loss (2–3 dB for the Py filters and 3–5 dB for the Fe filters) is also not strongly dependent on the width of the magnetic element. The power attenuation is close to 100 dB/cm for the Permalloy devices and dramatically larger for Fe, with values at the higher frequencies close to 180 dB/cm. Inside the stop-band the reflection coefficient is better than –15 dB. The stop-band frequency range for the Py filter is about 2 GHz, and for Fe it is about 6 GHz.

In Fig. 2, it is seen that the FMR frequency is nearly independent of the length of the microstrip. This is consistent with theoretical calculations because the  $N_y$  coefficient increases very slightly with an increase of line length. The increase of  $L$  does,

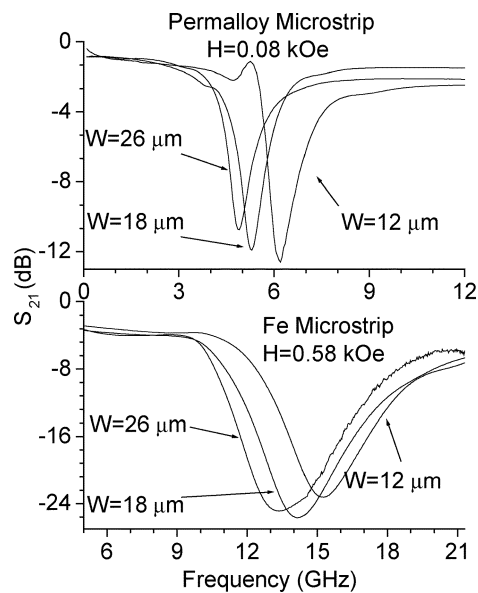


Fig. 1. Transmission response of 3.3 mm long Permalloy (upper panel) and Fe (lower panel) based stop-band filters as a function of frequency for different line-widths ( $W$ ) of the magnetic element.

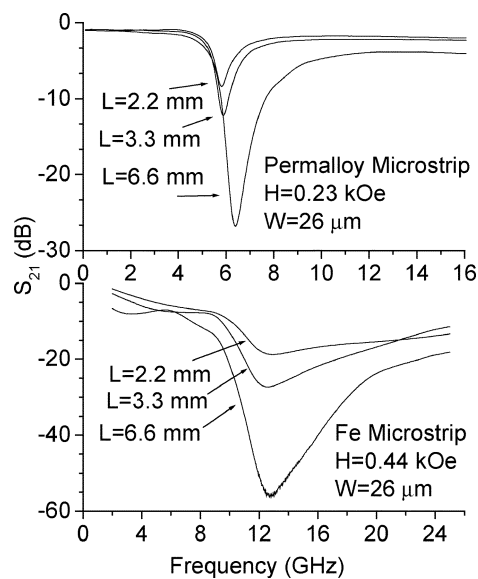


Fig. 2. Transmission parameter of 26  $\mu\text{m}$  wide Permalloy (upper panel) and Fe (lower panel) based stop-band filters as a function of frequency for different line-lengths ( $L$ ) of the magnetic element.

however, increase absorption as expected. Again, the linewidth does not follow a clear pattern as a function of thickness. However, the smallest linewidths seem to occur for the longest lines.

A comparison of experimental and theoretical FMR frequencies is given in Table I. The agreement for both the Fe and Py based devices is excellent when the width of the microstrip is changed. Also, as expected, the experimental results for the Fe-based devices do not show much variation of FMR frequency as a function of the line length. In contrast, a small but distinct

change in the FMR frequency is measured in the Py-based devices as the length is increased. This may be due to a slight nonuniformity in the applied field which would shift the frequency up slightly for a longer structure. Our experimental setup produced a biasing field which was nearly uniform over a distance of 2 mm. For the longer devices, with a length of 6 mm, the static magnetic field at the ends of the device was approximately 20% larger than the field at the center. Using (1), one can see that this small variation could lead to an increase in frequency as  $L$  is increased in the Py devices. Assuming an increase of 10% in the average field, the frequency would be increased by about 0.15 GHz and this explains some of the increase in frequency as the length is increased. We note that there is also a small increase in the longer Fe-based devices. If we also assume a 10% increase in the average field for the long Fe-based devices we obtain a frequency of 12.69 GHz, which matches the experimental result.

We note that for a given device, the width of the attenuation dip becomes distinctly narrower as the applied field is increased and the resonance moves to higher frequencies (data not shown). This behavior is surprising because one normally expects the effective damping in the spin equations of motion to be proportional to the frequency and the linewidth in an FMR experiment is proportional to the damping. This narrowing of the width of the attenuation peak is consistent with theoretical results [9] but will be explored in detail elsewhere.

#### IV. CONCLUSION

The use of Fe and Permalloy in microstrip filters demonstrates the feasibility of magnetically tunable stop-band planar microwave devices. The considerable enhancement of the resonance frequency of the device is achieved by narrowing the width ( $W$ ) of the magnetic film. Indeed, the resonance frequency is a function of the demagnetizing factors which are directly related to the width, length, and thickness of the device. This way of integrating Permalloy and Fe in guided wave structures opens the road to a new generation of miniature size low-cost tunable planar microwave devices.

#### REFERENCES

- [1] E. Schloemann *et al.*, *J. Appl. Phys.*, vol. 63, p. 3140, 1988.
- [2] C. S. Tsai *et al.*, *IEEE Trans Magn.*, vol. 35, p. 3178, 1999.
- [3] N. Cramer *et al.*, *J. Appl. Phys.*, vol. 87, p. 6911, 2000.
- [4] R. E. Camley and D. L. Mills, *J. Appl. Phys.*, vol. 82, pp. 3058–3067, 1997.
- [5] R. J. Astalos and R. E. Camley, *J. Appl. Phys.*, vol. 83, pp. 3744–3749, 1998.
- [6] B. Kuanr *et al.*, *J. Appl. Phys.*, vol. 93, p. 8591, 2003.
- [7] I. Hunyen *et al.*, *IEEE Microwave Guided Wave Lett.*, vol. 9, p. 1051, 1999.
- [8] E. Salahun *et al.*, *J. Appl. Phys.*, vol. 91, p. 5449, 2002.
- [9] B. Kuanr, Z. Celinski, and R. E. Camley, *Appl. Phys. Lett.*, vol. 83, p. 3969, 2003.
- [10] R. B. Marks, *IEEE Trans. Microwave Theory Tech.*, vol. 39, p. 1205, 1991.
- [11] C. Kittel, *Phys. Rev.*, vol. 73, p. 155, 1948.
- [12] A. Aharoni, *J. Appl. Phys.*, vol. 83, p. 3432, 1998.